Monooxygenase Activity of *Octopus vulgaris* Hemocyanin†

Kenji Suzuki, Chizu Shimokawa, Chiyuki Morioka, and Shinobu Itoh*

Department of Chemistry, Graduate School of Science, Osaka City University, 3-3-138 Sugimoto, Sumiyoshi-ku, Osaka 558-8585, Japan

Received February 17, 2008; Revised Manuscript Received April 28, 2008

ABSTRACT: *Octopus vulgaris* hemocyanin (*Ov*-Hc) and one of its minimal functional units (*Ov*-g) have been purified, and their spectroscopic features and monooxygenase (phenolase) activity have been examined in detail. The oxy forms of both *Ov*-Hc and *Ov*-g are stable in 0.5 M borate buffer (pH 9.0) even in the presence of a high concentration of urea at 25 °C; ∼90 and ∼75% of the (μ-η^2:η^2-peroxo)dicopper(II) species of *Ov*-Hc and *Ov*-g, respectively, remained unchanged after argon (Ar) gas flushing of the sample solutions for 1 h. The catalytic activity of *Ov*-g in the oxygenation reaction (multiturnover reaction) of 4-methylphenol (*p*-cresol) to 4-methyl-1,2-dihydroxybenzene (4-methylcatechol) was higher than that of *Ov*-Hc, and its catalytic activity was further accelerated by the addition of urea. Kinetic deuterium isotope effect analysis and Hammett analysis using a series of phenol derivatives under anaerobic conditions (single-turnover reaction) have indicated that the monooxygenation reaction of phenols to catechols by the peroxo species of oxyhemocyanin proceeds via electrophilic aromatic substitution mechanism as in the case of tyrosinase. The effect of urea on the redox functions of oxyhemocyanin is discussed on the basis of the spectroscopic analysis and reactivity studies.

Hemocyanin is the oxygen carrier protein in the hemolymph of many mollusks and arthropods (*1*). It is a large multisubunit protein whose structure varies significantly depending on the source of the protein (*2, 3*). Thus, arthropod hemocyanin subunits have a molecular mass of ∼75 kDa and associate into oligomers of hexamers in vivo, whereas molluscan hemocyanin subunits contain seven or eight oxygen-binding sites, termed functional units, and have a molecular mass of ∼400 kDa, which associate in multiples of 10 to form cylindrical supramolecular assemblies (*1–5*).

The active site structures of hemocyanins from various origins have so far been studied extensively by means of several spectroscopic methods and X-ray crystallographic analysis to demonstrate that a magnetically coupled dinuclear copper center supported by six histidine imidazole ligands (three histidines for each copper) is the common structural feature of the active sites of proteins (*1–4*). Thus, dioxygen is bound to the dicopper(I) site of deoxyhemocyanin (reduced form) to generate oxyhemocyanin (oxy form) involving a (μ-η^2:η^2-peroxo)dicopper(II) core structure as shown in Figure 1 (*6, 7*). The side-on peroxo dinuclear copper(II) (Cu_2O_2) core structure has also been found in the oxy forms of tyrosinase (EC 1.14.18.1) and catechol oxidase (EC 1.10.3.1) (*8–10*). Therefore, the oxy forms of these copper proteins exhibit very similar spectroscopic features that originate from the Cu_2O_2 unit, even though the overall structures of the proteins are quite different (*8, 11*).

Despite having the same side-on peroxo dicopper(II) species (Figure 1), these copper proteins exhibit different

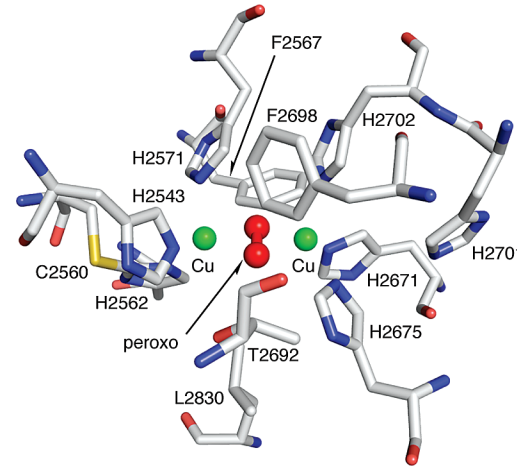

FIGURE 1: Active site structure of oxyhemocyanin from *Octopus dofleini* (Protein Data Bank entry 1JS8) (*6*).

chemical reactivity toward external substrates. Namely, tyrosinase catalyzes the ortho hydroxylation of phenols to the corresponding catechols, so-called phenolase activity (eq 1), as well as the oxidation of catechols to the corresponding *o*-quinones termed catecholase activity (eq 2) (*8, 12*). On the other hand, catechol oxidase exhibits only catecholase activity but shows no monooxygenase activity toward external substrates (*9*). In contrast to these dicopper enzymes, hemocyanin has essentially no redox reactivity toward external substrates but exhibits only reversible dioxygen binding ability in acting as the dioxygen storage and carrier protein (*1*).

In this respect, recent studies on the enzymatic functions of arthropod hemocyanins are worth noting. Beltramini and co-workers reported that arthropod hemocyanins isolated from crab *Carcinus maenas* and lobster *Homarus americanus*

† This study was financially supported in part by Grants-in-Aid for Scientific Research on Priority Area (18033045, 19020058, 19027048, and 19028055) from MEXT, Japan.

* To whom correspondence should be addressed. E-mail: shinobu@sci.osaka-cu.ac.jp. Phone and fax: +81-6-6605-2564.

10.1021/bi8002764 CCC: $40.75
Published on Web 06/14/2008

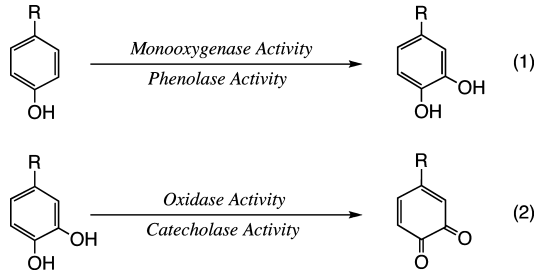

exhibited the catecholase activity, and their catalytic activity increased by 1.5- and 5-fold, respectively, when a certain amount of $NaClO_4$ was added to the solution (*13*). The authors suggested that perchlorate ions induce a conformational change in the protein, resulting in an increase in enzymatic activity (V_{max}). SDS[1] has also been demonstrated to exhibit a similar effect on the protein function (*14–16*). On the other hand, Decker and co-workers demonstrated that tarantula hemocyanin gained phenoloxidase activity after limited proteolysis with trypsin or chymotrypsin (*17, 18*). In this case, the proteolytic cleavage removes an N-terminal fragment to open the entrance for incorporation of the substrate. Söderhäll and co-workers reported a similar result using crayfish hemocyanin (*19*). Furthermore, horseshoe crab hemocyanin was shown to acquire catecholase activity when it was allowed to interact with an antimicrobial peptide (*20, 21*). In this case as well, the interaction with the peptide may induce a conformational change in hemocyanin that allows it to gain catalytic activity. However, the mechanism of the enzymatic functions of arthropod hemocyanins has yet to be addressed in detail.

In contrast to the numerous studies of arthropod hemocyanins, the enzymatic activity of molluscan hemocyanin has been investigated less. Hemocyanin isolated from *Octopus vulgaris* has been demonstrated to exhibit catecholase (oxidase) activity, for which a one-electron oxidation mechanism generating a semiquinone radical intermediate was suggested (*22*). However, monooxygenase (phenolase) activity of molluscan hemocyanin has yet to be examined in detail. In this study, we have investigated the monooxygenase (phenolase) activity of *O. vulgaris* hemocyanin (*Ov*-Hc) and its minimal functional unit g (*Ov*-g) containing just one dinuclear copper active site to gain further insight into the reactivity of (μ-η^2:η^2-peroxo)dicopper(II) species in biological systems (*23*).

EXPERIMENTAL PROCEDURES

Materials. All chemical reagents used in this study, except *p*-Br-C_6D_4OH, were commercial products of the highest available purity and used as received. The deuterated phenol derivative, *p*-Br-C_6D_4OH, was prepared according to the reported procedure (*24*), and its purity (>99%) was confirmed by ^{13}C NMR and MS analyses using JEOL FT-NMR Lambda 300WB and JEOL JMS-700T Tandem MS-station mass spectrometers, respectively. CD spectra were recorded on a JASCO J-820 spectrophotometer.

Purification of O. vulgaris Hemocyanin (Ov-Hc). Ov-Hc was isolated according to the reported procedure as follows (*25*). The hemolymph of *O. vulgaris* was collected from living animals purchased at Fukahiro fish dealer at Kuromon market in Osaka City, Japan. The blood cells were removed by brief low-speed centrifugation for 20 min at 27000*g* using a KUBOTA model 3700 micro cooled centrifuge. The clear supernatant was sedimented by centrifugation for 6 h at 120000*g* using a Hitachi model CP 70MX preparative ultracentrifuge. The sediment was dissolved in a small volume of 0.1 M Tris-HCl buffer (pH 8.0) and again sedimented by centrifugation for 13 h at 110000*g*. The sediment was then slowly resolved again in the same buffer and stored at 4 °C in a model MC-8EF2 chlomatochamber.

Isolation and Purification of Minimal Functional Unit g (Ov-g). Ov-g of *O. vulgaris* was isolated and purified by following the reported procedure for the isolation and purification of functional unit g of *O. dofleini* hemocyanin (*26*). Thus, *Ov*-g was removed from the native protein by limited proteolysis using V8 protease (staphylococcal serine protease, EC 3.4.21.19) in 0.05 M ammonium carbonate buffer (pH 8.0) at 37 °C for 24 h (enzyme/hemocyanin ratio of 10^{-4}) and isolated by ion-exchange column chromatography on a RESORCE Q column (volume of 6 mL) at 4 °C in 0.05 M Tris-HCl buffer (pH 8.9) with 0.01 M EDTA. Elution was carried out with a 0 to 0.4 M NaCl gradient using an ÄKTA prime plus (Figure S1 of the Supporting Information). The purity of the sample was confirmed by SDS−PAGE (inset of Figure S1).

Determination of the Concentration of the Oxy Form. The concentration of copper ion in an *Ov*-Hc solution was first determined by atomic absorption spectroscopy using a Horiba JOBIN YVON JY3BS instrument. Then, the UV−vis spectrum of that solution was measured with a Jasco UV−vis−NIR spectrophotometer (V-550) in 0.1 M Tris-HCl buffer (pH 8.0) under oxygen-saturated conditions. From the results described above, the molar absorption coefficient at 580 nm [for the (μ-η^2:η^2- peroxo)dicopper(II) form] was determined to be 932 M^{-1} cm^{-1}. The level of the oxy form of *Ov*-Hc was evaluated from the absorbance ratio A_{348}/A_{280}, the value of 0.22 corresponding to 100% oxyhemocyanin at pH 8.0.

Monitoring the O_2 Concentration. The time courses of O_2 concentration changes were monitored by a Clark-type oxygen electrode connected to a closed cell (Central Kagaku Co. Ltd.). The applied potential was −0.6 V versus Ag/AgCl/KCl (1.0 M). The measurement of the oxygen consumption rate was performed at room temperature in 0.5 M borate buffer (pH 9.0) under air-saturated conditions.

Product Analysis. Products of each reaction were analyzed with a HPLC system consisting of a Shimadzu LC-6A chromatographic pump and an on-line Shimadzu UV−vis spectrophotometric detector. An ODS column (Prodigi, 250 mm × 4.6 mm, Phenomenex) was used for the HPLC separation at room temperature with a mobile phase (65:35 acetonitrile/water mixture, containing 0.1% trifluoroacetic acid) at a constant flow rate of 0.3 mL/min.

RESULTS AND DISCUSSION

Characterization of Ov-Hc and Ov-g. Hemocyanins from *O. vulgaris* and *O. dofleini* form a gigantic supramolecular

[1] Abbreviations: *Ov*-Hc, *Octopus vulgaris* hemocyanin; *Ov*-g, functional unit g of *O. vulgaris* hemocyanin; SDS, sodium dodecyl sulfate; CD, circular dichroism; EDTA, ethylenediaminetetraacetic acid; HPLC, high-performance liquid chromatography; ODS, octadecyl sulfate; UV−vis, ultraviolet−visible; LMCT, ligand-to-metal charge transfer; DOPA, 3,4-dihydroxy-L-phenylalanine.

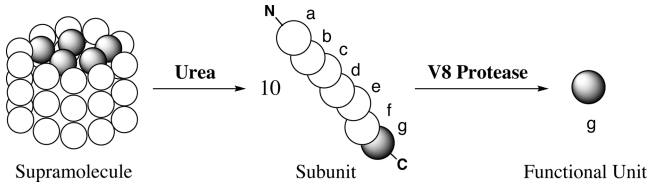

FIGURE 2: Schematic representations of the quaternary structure, subunit, and functional unit g of octopus hemocyanin.

assembly having a cylindrical shape with a diameter of ~350 Å as illustrated in Figure 2 (*2, 5, 25, 27–29*). The supramolecular assembly consists of 10 subunits, each of which contains seven oxygen binding functional units called a, b, c, d, e, f, and g (Figure 2). Thus, there are a total of 70 oxygen-binding dinuclear copper sites in the supramolecular assembly.

It has also been reported that each subunit of *Ov*-Hc can be dissociated from the supramolecular assembly via treatment with a high concentration of urea as illustrated in Figure 2 (*30*). Furthermore, minimal functional unit g existing at the C-terminal domain of *O. dofleini* hemocyanin can be removed and isolated from the subunit by the treatment with a hydrolytic enzyme such as V8 protease (*5, 6, 26*). Therefore, in this study, the monooxygenase (phenolase) activity of *O. vulgaris* hemocyanin was examined by using native protein (*Ov*-Hc) and its functional unit g (*Ov*-g) both in the presence and in the absence of urea.

Native *Ov*-Hc exhibits an intense absorption band at 348 nm together with an additional weak band at 580 nm in 0.5 M borate buffer at pH 9.0 (Figure S2, solid line; also see Figure 5). These two bands have been assigned as peroxo-to-copper(II) charge transfer (LMCT) transitions of the (μ-η^2:η^2-peroxo)dicopper(II) species (*11*). The intensity of the LMCT bands increased only slightly (~5%), when O_2 gas was flushed on the sample solution for 30 min, indicating that most of the dinuclear copper site (~95%) of the native hemocyanin is saturated with O_2 even under air. Notably, the (μ-η^2:η^2-peroxo)dicopper(II) species of oxyhemocyanin also remained unchanged, even if the sample was kept standing under anaerobic conditions (argon gas flushing) as demonstrated in the inset of Figure S2 (solid line). These results clearly indicate that the O_2 affinity of native *Ov*-Hc is fairly strong under the experimental conditions.

In the presence of a high concentration of urea (8 M), an ordinary protein denaturant, the spectrum of the oxy form (dashed line in Figure S2) was hardly affected, but the intensity at 348 nm decreased slightly (the dashed line in the inset of Figure S2). As stated above, addition of urea to a solution of native hemocyanin induces dissociation of the subunits from the supramolecular assembly (Figure 2) (*30*). Thus, the slow decrease in the intensity of the absorption band of the peroxo species of *Ov*-Hc may indicate that the O_2 affinity in the dissociated subunits becomes a little weaker.

The minimal functional unit *Ov*-g detached from the C-terminal domain of the subunit via treatment with V8 protease also exhibits an intense LMCT band at 348 nm together with a weak LMCT band at 572 nm (Figure S3; also see Figure 8). Also in this case, the peroxo species of *Ov*-g was quite stable under anaerobic conditions; the absorbance at 348 nm did not change for 1 h (solid line in the inset of Figure S3). On the other hand, the destabilizing effect of urea on the peroxo species was somehow stronger in the case of *Ov*-g as compared to the case of native *Ov*-Hc; the decrease in the intensity of the absorption band at 348 nm after 1 h was ~25 and ~10% for *Ov*-g and *Ov*-Hc, respectively (see the dashed lines in the insets of Figures S2 and S3).

The CD spectra of *Ov*-Hc in the absence (solid line) and presence (dashed line) of urea are shown in Figure 3 (left). The spectral shape in the absence of urea is nearly the same as that of the reported spectrum (*26, 31*). The several weak bands in the visible region shown in the inset of Figure 3 are characteristic of the oxyhemocyanin, since these bands are absent in the deoxy form and the met form of hemocyanin (*31*). The presence of two negative minima at 208 and 220 nm is characteristic of proteins with both α and β structures. The CD of the subunit has a more intense band at 208 nm than at 220 nm, and this is one of the characteristics of $\alpha+\beta$-type proteins. The spectral shape of *Ov*-Hc in the presence of urea (dashed line) is almost the same as that measured in the absence of urea (solid line). Thus, it can be concluded that the three-dimensional structure of the subunits in the supramolecular assembly is the same as that of the dissociated subunit in the presence of urea.

The CD spectra of *Ov*-g in the absence (solid line) and presence (dashed line) of urea are shown in Figure 3 (right). The spectral shape in the visible region is nearly identical to those of the native hemocyanin both in the absence (solid line) and in the presence (dashed line) of urea. The similarity of the spectra in the visible region supports the notion that the Cu_2O_2 (dicopper-peroxo) core structure of the oxy form is maintained in all the cases, which has been demonstrated by the UV−vis spectra (Figures S2 and S3). With respect to the bands at ~200 nm, the relative intensity of the 208 nm band to that of the 220 nm band of *Ov*-g in the absence of urea becomes smaller than that of the native protein as reported previously (*26*). Notably, addition of a high concentration of urea resulted in an increase of the relative intensity of the 208 nm band against the 220 nm band. This result clearly indicates that the content of α and β structures in *Ov*-g was changed by the interaction with urea, although the details about the structural change are not clear at present.

Monooxygenase (Phenolase) Activity (Multiturnover Catalytic Reaction under Aerobic Conditions). Neither the native *Ov*-Hc nor *Ov*-g exhibited catalytic activity for the oxidation of tyrosine and DOPA, the native substrates for tyrosinase. This may be due to the hydrophobic environment of the active site pocket of the proteins, which consists of Phe2567, Phe2698, Lue2830, and Thr2692 (see Figure 1). The highly polar amino acid substrates containing the ionic groups (NH_3^+ and COO^-) may resist being in such a hydrophobic space near the Cu_2O_2 core. On the other hand, simple catechols such as 1,2-dihydroxybenzene (catechol) and 4-methyl-1,2-dihydroxybenzene (4-methylcatechol) can be oxidized to the corresponding *o*-quinones (catecholase activity) by native *Ov*-Hc (*22*). These simple catechol derivatives may be able to enter the active site pocket, because they do not have such highly polar ionic functional groups. On the basis of these results, we decided to investigate the monooxygenation activity (phenolase activity) of *Ov*-Hc by using simple phenol derivatives (*23*).

Thus, catalytic reaction of 4-methylphenol was first examined in a 0.5 M borate buffer solution (pH 9.0) containing NH_2OH (8.5 mM) at 25 °C and was followed by

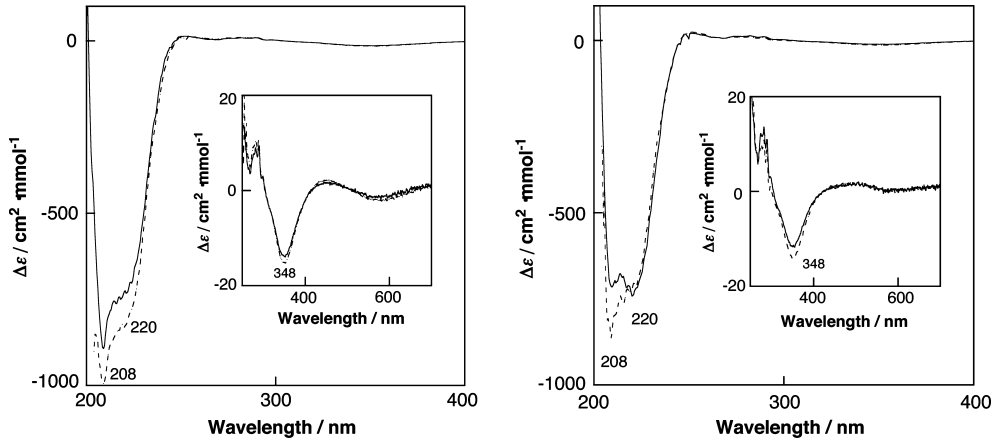

FIGURE 3: Circular dichroism of *Ov*-Hc (0.02 mM) (left) and *Ov*-g (0.02 mM) (right) in 0.5 M borate buffer (pH 9.0) in the absence (solid line) and presence (dashed line) of urea (8 M) at room temperature under air.

Scheme 1: Simplified Catalytic System of Phenolase Reaction of *Ov*-Hc (*32*)

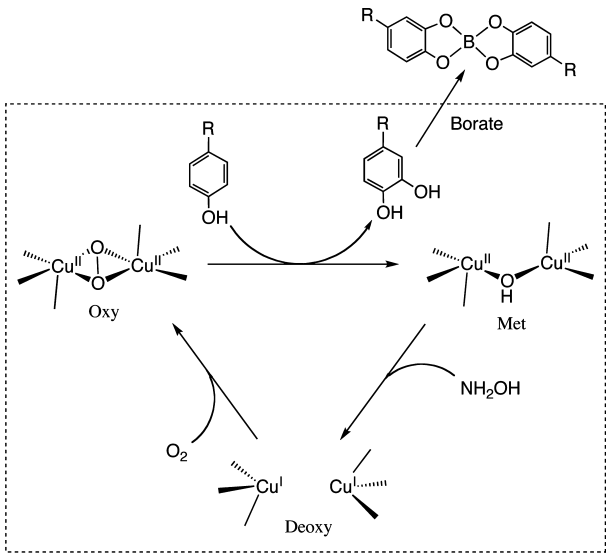

monitoring the O_2 consumption rate using an ordinary Clark-type oxygen electrode connected to a closed cell. We have developed this system to examine the phenolase activity of tyrosinase without interference from its catecholase activity as indicated in Scheme 1 (*32*). Namely, borate anion of the buffer solution acts as the trapping agent of the primary oxygenation product catechols and prevents the overoxidation of catechols to the corresponding *o*-quinones (catecholase activity). This simplifies the catalytic cycle very much, since the protection of the catecholase activity shuts down the following complicated side reactions such as formation of nonenzymatic melanin pigment from the *o*-quinone products (*33*). In this particular system, however, the reduction of the met form, generated by the reaction of the oxy form and phenol substrates, does not proceed because of the absence of the native electron donor catechols, which is excluded from the catalytic cycle by formation of the complex with borate anion. Thus, to reconstruct the reduction process from the met form to the deoxy form, we used NH_2OH as an external sacrificial reductant. This actually worked very well to give 4-methylcatechols as the major product (92% based on the extent of O_2 consumption) (Figure S4).

The time courses of O_2 comsumption during the catalytic reactions are shown in Figure 4. The reaction proceeded

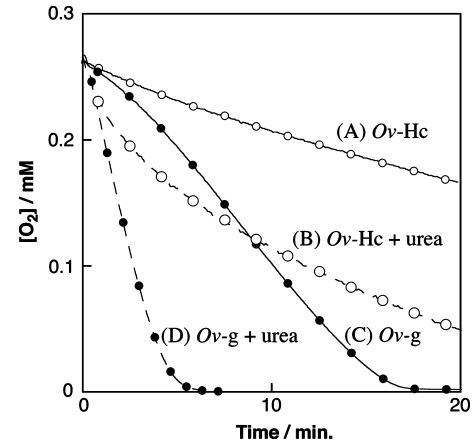

FIGURE 4: Time courses of O_2 concentration changes during the catalytic oxidation of 4-methylphenol (9.9 mM) by *Ov*-Hc (0.01 mM) in the absence (A) and presence (B) of urea (6 M) and also by *Ov*-g (0.01 mM) in the absence (C) and presence (D) of urea (6 M) in 0.5 M borate buffer (pH 9.0) containing NH_2OH (5.1 M) at room temperature.

slowly with native *Ov*-Hc (line A), where the initial maximum rate was 0.11 μM/s. Addition of urea (6 M) to the system accelerated the initial rate as 0.39 μM/s, whereas the reaction gradually slowed after 5 min (line B). On the other hand, *Ov*-g itself exhibited a higher catalytic activity (0.31 μM/s) (line C) as compared to native *Ov*-Hc, and the reaction proceeded continuously until all molecular oxygen was consumed (~18 min). More interestingly, upon addition of 6 M urea, the catalytic activity of *Ov*-g further increased to 1.1 μM/s (line D), and the turnover number reached ~5 min^{-1}. Recently, Gielens and co-workers reported that the catecholase activity of molluscan hemocyanin was moderately enhanced by limited proteolysis with subtilisin, where some of the functional units exhibiting the enzymatic activity were identified (*34, 35*).

From these results, the following conclusions can be drawn. Isolated *Ov*-g exhibits a higher catalytic activity for the monooxygenation reaction of phenols as compared to native *Ov*-Hc (compare lines A and C and lines B and D). The accessibility of the substrate to the Cu_2O_2 reaction center may become much easier in *Ov*-g than in *Ov*-Hc, because a relatively large portion of the functional units is buried in the native supramolecular assembly of *Ov*-Hc as illustrated in Figure 2. Addition of urea to the system induces the dissociation of the subunits into the solution (*30*), thus

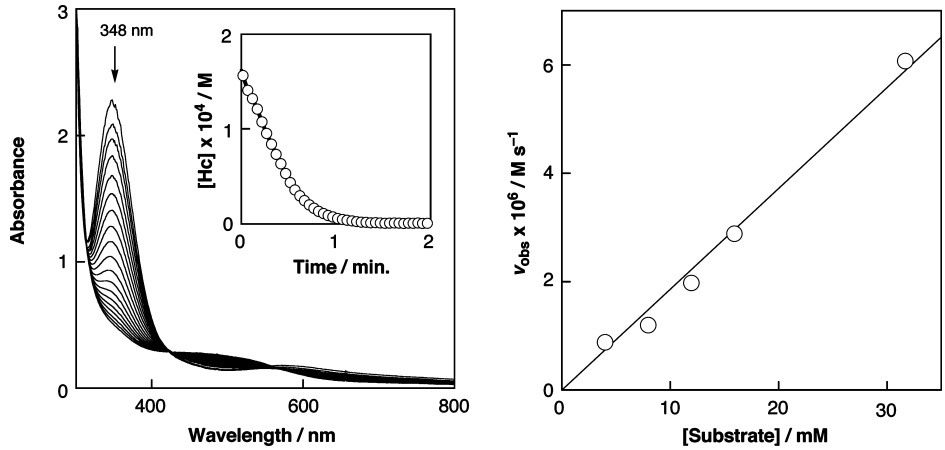

FIGURE 5: Spectral change observed upon addition of *p*-methylphenol (16 mM) to the oxy form of *Ov*-Hc (0.17 mM) in 0.5 M borate buffer (pH 9.0) containing 10% MeOH and 8 M urea at 25 °C under Ar: 3 s interval (inset, time course of the absorption change at 348 nm) (left) and plot of v_{obs} vs substrate concentration (right).

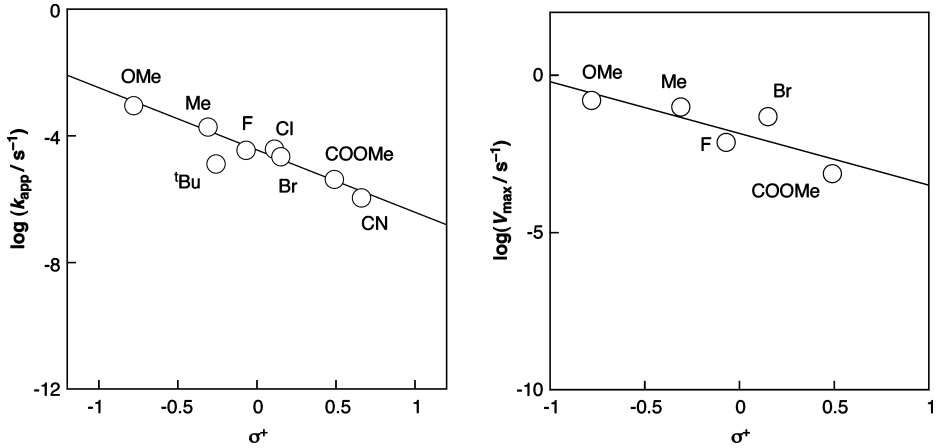

FIGURE 6: Hammett plots for the oxygenation of phenols by the oxy form of *Ov*-Hc (left) and by the oxy form of *Ov*-g (right). The data are taken from Tables S1 and S2, respectively.

enhancing the accessibility of the substrate into the active site of *Ov*-Hc (compare lines A and B). Notably, the catalytic activity of *Ov*-g was further accelerated by the addition of urea (compare lines C and D). This clearly indicates that the interaction of urea with *Ov*-g induces some conformational change in the protein and opens the entrance for the substrate to get into the reaction center. In fact, Betzel and co-workers reported that a slight movement of the C-terminal part of the functional unit from gastropod hemocyanin provides an open look into the dinuclear copper active site (*36*). The occurrence of such a conformational change in the protein of *Ov*-g was suggested by the CD spectral change upon addition of urea to *Ov*-g (Figure 3, right). In the next section, mechanistic details of the monooxygenase activity of the oxy form of *Ov*-Hc and *Ov*-g are addressed in detail.

Mechanism of Monooxygenase (Phenolase) Activity (Single-Turnover Reaction under Anaerobic Conditions). Addition of an excess of *p*-cresol (4-methylphenol) (16 mM) to a borate buffer solution of the oxy form of *Ov*-Hc (0.17 mM) containing 8 M urea at 25 °C resulted in a decrease in the intensity of the absorption bands of the peroxo species as shown in Figure 5 (left). The reaction was complete in <1 min, and the corresponding catechol (4-methyl-1,2-hydroxylbenzene) was obtained nearly quantitatively (confirmed by HPLC). In the absence of urea, the spectral change was much slower as shown in Figure S5. As discussed above, addition of urea to the system may cause not only the dissociation of the subunits from the supramolecular assembly (Figure 2) but also a partial conformational change in the protein to open an entrance for substrate (phenol) incorporation.

From the initial slope of the time course of the reaction shown in the inset of Figure 5, the apparent rate constant v_{obs} was determined to be 1.2×10^{-6} M/s. Then, the dependence of the rate on the substrate concentration was examined to obtain a linear correlation as shown in Figure 5 (right). Thus, the apparent first-order rate constant (k_{app}) was determined to be 1.9×10^{-4} s^{-1} from the slope. Similar spectral changes were obtained with a series of phenol derivatives as demonstrated in Figures S6−S12 (left), and their apparent first-order rate constants (k_{app}) were determined from the slopes of the linear correlation in the plots of v_{obs} versus the substrate concentrations as presented in Figures S6−S12 (right). The kinetic data thus obtained are summarized in Table S1.

The linear dependence of v_{obs} on the substrate concentration (Figure 5, right) may indicate that binding of the substrate to the oxy form of *Ov*-Hc is weak. This is reasonable, because hemocyanin is essentially an oxygen carrier protein, and not a monooxygenase. Thus, the substrate binding to the active site of *Ov*-Hc is rather weak compared to that of tyrosinase, which shows a typical Michaelis−

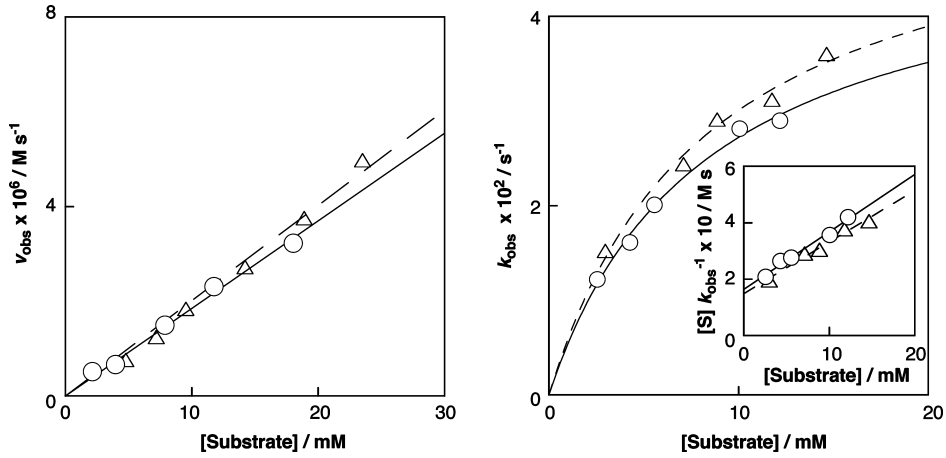

FIGURE 7: Plot of v_{obs} vs substrate concentration for the oxygenation of *p*-Br-C_6H_4OH (○) and *p*-Br-C_6D_4OH (△) by the oxy form of *Ov*-Hc (left) and plot of k_{obs} vs substrate concentration for the oxygenation of *p*-Br-C_6H_4OH (○) and *p*-Br-C_6D_4OH (△) by the oxy form of *Ov*-g. The inset is a Hanes−Woolf plot.

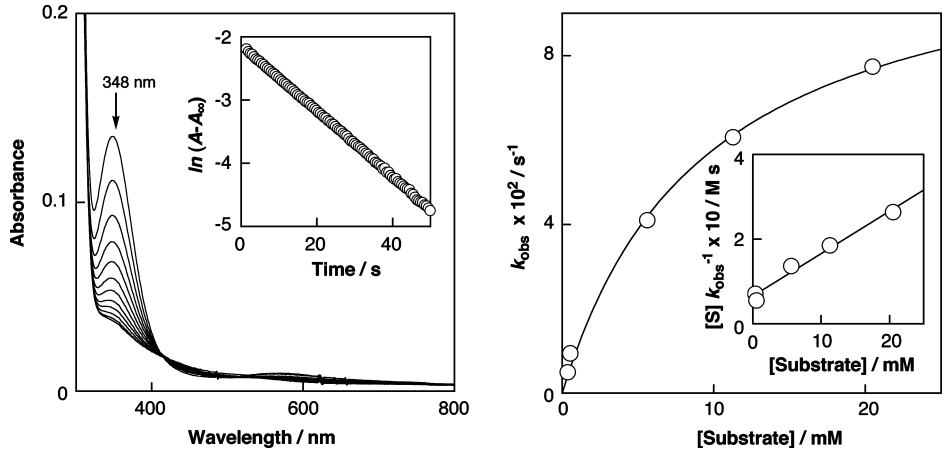

FIGURE 8: Spectral change observed upon addition of *p*-methylphenol (11.3 mM) to the oxy form of *Ov*-g in 0.5 M borate buffer (pH 9.0) containing 8 M urea at 25 °C under Ar: 5 s interval (inset, first-order plot based on the absorption change at 348 nm) (left) and plot of k_{obs} vs substrate concentration (inset, Hanes−Woolf plot for the reaction) (right).

Menten-type saturation kinetics due to the strong substrate binding (*32*).

To gain insight into the mechanism of oxygenation of phenols by the oxyhemocyanin, electronic effects of the substituents of the substrates on the reaction rate were examined as shown in Figure 6 (left). The plot of log k_{app} against the Hammett σ^+ gave a linear correlation, from which a Hammett ρ constant of −2.0 was obtained. It should be emphasized that the ρ value of this reaction is quite similar to that of the phenolase activity of mushroom tyrosinase ($\rho = -2.4$) reported previously (*32*). The good agreement in the Hammett ρ values between the two systems strongly suggests that the oxygenation of phenols by the oxyhemocyanin involves the same mechanism as that of phenolase activity of tyrosinase, that is, the electrophilic aromatic substitution mechanism illustrated in Scheme 2 (*37–39*). Namely, the reaction starts from the coordination of phenolate substrate to one of the copper(II) ions of peroxo complex **A** to give intermediate **B** and following electrophilic attack by the peroxo moiety to the aromatic ring of the substrate induces the formation of the C−O bond, giving intermediate **C**. Then, proton migration readily occurs to give final product **D**, the catechol complex of met-hemocyanin.

In support of this mechanism, a negative kinetic deuterium effect (KIE = 0.9) was obtained, when *p*-Br-C_6D_4OH was used instead of *p*-Br-C_6H_4OH (Figure 7, left). This clearly indicates that the migration of the proton from the ortho position of the substrate (**C** to **D**) is not involved in the rate-determining step; instead, the rate-limiting step involves the conversion of the aromatic sp^2 carbon to an sp^3 carbon (**B** to **C**).

Scheme 2: Mechanism of the Monooxygenation Reaction of Phenols to Catechols by Oxyhemocyanin

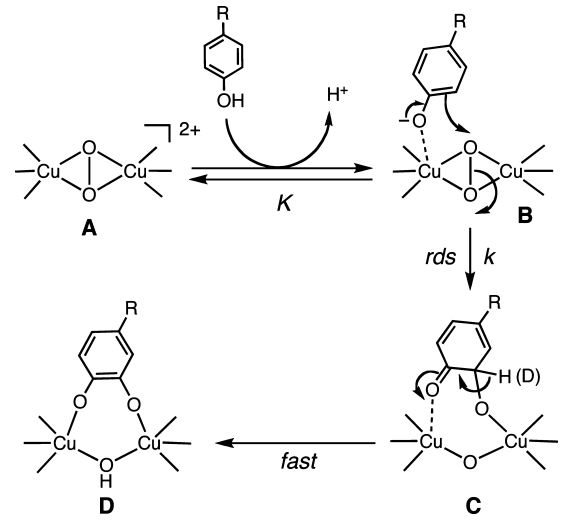

The monooxygenase activity of *Ov*-g was also examined under the same experimental conditions [in 0.5 M borate buffer (pH 9.0) containing 8 M urea at 25 °C under argon]. Figure 8 (left) shows the spectral change observed upon addition of *p*-methylphenol (11.3 mM) to the oxy form of *Ov*-g (12 μM). In this case as well, the (μ-η^2:η^2-peroxo)dicopper(II) species of *Ov*-g exhibiting the intense absorption band at 348 nm readily disappeared, and from the final reaction mixture, the corresponding catechol was obtained as the major product (confirmed by HPLC). Nonetheless, there are some notable differences in the kinetic behavior between the native *Ov*-Hc and isolated *Ov*-g. For example, the time course of the decay of the peroxo species of *Ov*-g obeys the first-order rate law as shown in the inset of Figure 8 (also see Figures S13−S16, left), whereas that of native *Ov*-Hc does not (more like a zeroth-order; see the inset of Figure 5, left). Thus, the pseudo-first-order rate constant (k_{obs}) was determined by the ordinary first-order plot shown in the inset of Figure 8. Moreover, the plot of k_{obs} versus substrate concentration for the *Ov*-g system exhibited a Michaelis−Menten-type saturation curve as shown in Figure 8 (right) (also see Figures S13−S16, right), which is also different from the linear dependence of the rate constant v_{obs} on the substrate concentration in the case of the native protein (Figure 5, right). These curious differences in the kinetic behavior between *Ov*-g and *Ov*-Hc can be explained as follows.

In the case of native *Ov*-Hc, the large subunit contains seven functional units from a to g (Figure 2), and the reactivity of each functional unit may be somewhat different. In such a case, the time course of the reaction may not be so simple, thus not following the simple first-order kinetics. With respect to the substrate binding to the active site pocket, aggregation of each functional unit in the large subunit may prohibit the smooth incorporation of the substrate into the active site of protein. Thus, the binding constant of the substrate in the native hemocyanin system may be quite small, affording the linear correlation between the rate constant and the substrate concentration as experimentally observed (Figure 5, right). On the other hand, the small *Ov*-g may behave as a simple unimolecule, thus exhibiting normal first-order kinetics. Furthermore, the prevention of substrate binding by subunit aggregation in the native protein may be largely diminished in the case of *Ov*-g, thus exhibiting the stronger binding of the substrates. As a result, the reaction showed the Michaelis−Menten kinetics (Figure 8, right).

In this case as well, the reaction rate increased as the electron donating ability of the para substituent of phenols is strengthened, as listed in Table S2, and Hammett analysis (Figure 6, right; plot of log k_{obs} vs σ^+) gave a Hammett ρ value of −1.6. In addition, there was also a negative kinetic deuterium isotope effect of 0.9, when *p*-Br-C_6D_4OH was employed instead of *p*-Br-C_6H_4OH (Figure 7, right). All these results clearly indicate that the reaction mechanism of the monooxygenase (phenolase) activity of *Ov*-g is the same as that of native *Ov*-Hc, that is, electrophilic aromatic substitution mechanism illustrated in Scheme 2. Thus, the intrinsic reactivity of the (μ-η^2:η^2-peroxo)dicopper(II) species of *Ov*-g is the same as that of *Ov*-Hc.

In summary, we have found that the oxygen carrier protein hemocyanin of *O. vulgaris* (*Ov*-Hc) exhibits monooxygenase (phenolase) activity toward simple phenols to give catechol products. Addition of a relatively high concentration of urea enhances the catalytic activity of *Ov*-Hc. Moreover, the catalytic activity of one of the functional units (*Ov*-g) of the *Ov*-Hc subunit is much higher than that of the parent protein in the presence of urea. Dissociation of functional unit g from the native protein and the interaction with urea may induce some conformational change around the active site pocket, enhancing the accessibility of the substrates to the Cu_2O_2 reaction center (*36*). The oxy forms of both *Ov*-Hc and *Ov*-g are stable enough to be examined in the single-turnover reaction under anaerobic conditions. Detailed kinetic analysis, including the kinetic deuterium isotope effect, and Hammett analysis using a series of phenol derivatives have indicated that the monooxygenation reaction of phenols to catechols by the peroxo species of both *Ov*-g and *Ov*-Hc proceeds via an electrophilic aromatic substitution mechanism as in the case of tyrosinase (*37*–*39*). Thus, the intrinsic reactivity of the (μ-η^2:η^2-peroxo)dicopper(II) species of hemocyanin is the same as that of tyrosinase.

ACKNOWLEDGMENT

We acknowledge Professor Shigenori Aono of the Okazaki Institute of Integrative Bioscience for his continuous helpful discussion.

SUPPORTING INFORMATION AVAILABLE

Elution diagram of *Ov*-Hc after digestion with V8 protease with ion-exchange column chromatography and SDS−PAGE of purified *Ov*-g (Figure S1), UV−vis spectra of *Ov*-Hc and *Ov*-g (Figures S2 and S3), product analysis by HPLC (Figure S4), spectral changes and kinetic analysis for the oxygenation reactions of para-substituted phenols by *Ov*-Hc and *Ov*-g (Figures S5−S16), and summary of the rate constants (Tables S1 and S2). This material is available free of charge via the Internet at http://pubs.acs.org.

REFERENCES

1. van Holde, K. E., and Miller, K. I. (1995) Hemocyanins. *Adv. Protein Chem. 47*, 1–81.
2. van Holde, K. E., Miller, K. I., and Decker, H. (2001) Hemocyanins and invertebrate evolution. *J. Biol. Chem. 276*, 15563–15566.
3. Magnus, K. A., Ton-That, H., and Carpenter, J. E. (1994) Recent structural work on the oxygen transport protein hemocyanin. *Chem. Rev. 94*, 727–735.
4. Jaenicke, E., and Decker, H. (2004) Functional changes in the family of type 3 copper proteins during evolution. *ChemBioChem 5*, 163–169.
5. Miller, K. I., Schabtach, E., and van Holde, K. E. (1990) Arrangement of subunits and domains within the *Octopus dofleini* hemocyanin molecule. *Proc. Natl. Acad. Sci. U.S.A. 87*, 1496–1500.
6. Cuff, M. E., Miller, K. I., van Holde, K. E., and Hendrickson, W. A. (1998) Crystal structure of a functional unit from octopus hemocyanin. *J. Mol. Biol. 278*, 855–870.
7. Magnus, K. A., Hazes, B., Ton-That, H., Bonaventura, C., Bonaventura, J., and Hol, W. G. J. (1994) Crystallographic analysis of oxygenated and deoxygenated states of arthropod hemocyanin shows unusual differences. *Proteins 19*, 302–309.
8. Solomon, E. I., Sundaram, U. M., and Machonkin, T. E. (1996) Multicopper oxidases and oxygenases. *Chem. Rev. 96*, 2563–2605.
9. Gerdemann, C., Eicken, C., and Krebs, B. (2002) The crystal structure of catechol oxidase: New insight into the function of type-3 copper proteins. *Acc. Chem. Res. 35*, 183–191.
10. Matoba, Y., Kumagai, T., Yamamoto, A., Yoshitsu, H., and Sugiyama, M. (2006) Crystallographic evidence that the dinuclear copper center of tyrosinase is flexible during catalysis. *J. Biol. Chem. 281*, 8981–8990.

11. Solomon, E. I., Chen, P., Mets, M., Lee, S.-K., and Palmer, A. E. (2001) Oxygen binding, activation, and reduction to water by copper proteins. *Angew. Chem., Int. Ed. 40*, 4570–4590.
12. Sánchez-Ferrer, A., Rodríguez-López, J. N., Francisco García-Cánovas, F., and García-Carmona, F. (1995) Tyrosinase: A comprehensive review of its mechanism. *Biochim. Biophys. Acta 1247*, 1–11.
13. Zlateva, T., Di Muro, P., Salvato, B., and Beltramini, M. (1996) The *o*-diphenol oxidase activity of arthropod hemocyanin. *FEBS Lett. 384*, 251–254.
14. Decker, H., Ryan, M., Jaenicke, E., and Terwilliger, N. (2001) SDS-induced phenoloxidase activity of hemocyanins from *Limulus polyphemus*, *Eurypelma californicum*, and *Cancer magiste*. *J. Biol. Chem. 276*, 17796–17799.
15. Pless, D. D., Aguilar, M. B., Falcón, A., Lozano-Alvarez, E., and Heimer de la Contera, E. P. (2003) Latent phenoloxidase activity and N-terminal amino acid sequence of hemocyanin from *Bathynomus giganteus*, a primitive crustacean. *Arch. Biochem. Biophys. 409*, 402–410.
16. Baird, S., Kelly, S. M., Price, N. C., Jaenicke, E., Meesters, C., Nillius, D., Decker, H., and Nairn, J. (2007) Hemocyanin conformational changes associated with SDS-induced phenol oxidase activation. *Biochim. Biophys. Acta 1774*, 1380–1394.
17. Decker, H., and Rimke, T. (1998) Tarantula hemocyanin shows phenoloxidase activity. *J. Biol. Chem. 273*, 25889–25892.
18. Decker, H., and Tuczek, F. (2000) Tyrosinase/catecholoxidase activity of hemocyanin: Structural basis and molecular mechanism. *Trends Biochem. Sci. 25*, 392–397.
19. Lee, S. Y., Lee, B. L., and Söderhäll, K. (2004) Processing of crayfish hemocyanin subunits into phenoloxidase. *Biochem. Biophys. Res. Commun. 322*, 490–496.
20. Nagai, T., Osaki, T., and Kawabata, S. (2001) Functional conversion of hemocyanin to phenoloxidase by horseshoe crab antimicrobial peptides. *J. Biol. Chem. 276*, 27166–27170.
21. Nagai, T., and Kawabata, S. (2000) A link between blood coagulation and prophenol oxidase activation in arthropod host defense. *J. Biol. Chem. 275*, 29264–29267.
22. Salvato, B., Santamaria, M., Beltramini, M., Alzuet, G., and Casella, L. (1998) The enzymatic properties of *Octopus vulgaris* hemocyanin: *o*-Diphenol oxidase activity. *Biochemistry 37*, 14065–14077.
23. Morioka, C., Tachi, Y., Suzuki, S., and Itoh, S. (2006) Significant enhancement of monooxygenase activity of oxygen carrier protein hemocyanin by urea. *J. Am. Chem. Soc. 128*, 6788–6789.
24. Das, B., Venkateswarlu, K., Majhi, A., Siddaiah, V., and Ravinder, R. (1990) A facile nuclear bromination of phenols and anilines using NBS in the presence of ammonium acetate as a catalyst. *J. Mol. Catal. A: Chem. 267*, 30–33.
25. Lambert, O., Boisset, N., Penczek, P., Lamy, J., Tavezu, J.-C., Frank, J., and Lamy, J. N. (1994) Quaternary structure of *Octopus vulgaris* hemocyanin. Three-dimensional reconstruction from frozen-hydrated specimens and intramolecular location of functional unit Ove and Ovb. *J. Mol. Biol. 238*, 75–87.
26. Miller, K. I., van Holde, K. E., Toumadje, A., Johnson, W. C., Jr., and Lamy, J. (1988) Structure and function of the carboxyl-terminal oxygen-binding domain from the subunit of *Octopus dofleini* hemocyanin. *Biochemistry 27*, 7282–7288.
27. Lamy, J., Leclerc, M., Sizaret, P.-Y., Lamy, J., Miller, K. I., McParland, R., and van Hold, K. E. (1987) *Octopus dofleini* hemocyanin: Structure of the seven-domain polypeptide chain. *Biochemistry 26*, 3509–3518.
28. van Holde, K. E., Miller, K., Schabtach, E., and Libertini, L. (1991) Assembly of *Octopus dofleini* hemocyanin. A study of the kinetics by sedimentation, light scattering and electron microscopy. *J. Mol. Biol. 217*, 307–321.
29. Lamy, J., Gielens, C., Lambert, O., Taveau, J. C., Motta, G., Loncke, P., De Geest, N., Préaux, G., and Lamy, J. (1993) Further approaches to the quaternary structure of octopus hemocyanin: A model based on immunoelectron microscopy and image processing. *Arch. Biochem. Biophys. 305*, 17–29.
30. Salvato, B., Ghiretti-Magaldi, A., and Ghiretti, F. (1979) Hemocyanin of *Octopus vulgaris*. The molecular weight of the minimal functional subunit in 3 M urea. *Biochemistry 18*, 2731–2736.
31. Takesada, H., and Hamaguchi, K. (1967) Circular dichroism of hemocyanin. *J. Biochem. 63*, 725–729.
32. Yamazaki, S., and Itoh, S. (2003) Kinetic evaluation of phenolase activity of tyrosinase using simplified catalytic reaction system. *J. Am. Chem. Soc. 125*, 13034–13035.
33. Land, E. J., Ramsden, C. A., and Riley, P. A. (2003) Tyrosinase autoactivation and the chemistry of ortho-quinone amines. *Acc. Chem. Res. 36*, 300–308.
34. Siddiqui, N. I., Préaux, G., and Gielens, C. (2004) Intrinsic and induced o-diphenoloxidase activity of b-hemocyanin of *Helix pomatia*. *Mircon 35*, 91–92.
35. Siddiqui, N. I., Akosung, R. F., and Gielens, C. (2006) Location of intrinsic and inducible phenoloxidase activity in molluscan hemocyanin. *Biochem. Biophys. Res. Commun. 348*, 1138–1144.
36. Perbandt, M., Guthöhrlein, E. W., Rypniewski, W., Idakieva, K., Stoeva, S., Voelter, W., Genov, N., and Betzel, C. (2003) The structure of a functional unit from the wall of a gastropod hemocyanin offers a possible mechanism for cooperativity. *Biochemistry 42*, 6341–6346.
37. Itoh, S., Kumei, H., Taki, M., Nagatomo, S., Kitagawa, T., and Fukuzumi, S. (2001) Oxygenation of phenols to catechols by a (μ-η^2:η^2-peroxo)dicopper(II) complex. Mechanistic insight into the phenolase activity of tyrosinase. *J. Am. Chem. Soc. 123*, 6708–6709.
38. Decker, H., Dillinger, R., and Tuczek, F. (2000) How does tyrosinase work? Recent insights from model chemistry and structural biology. *Angew. Chem., Int. Ed. 39*, 1591–1595.
39. Decker, H., Schweikardt, T., and Tuczek, F. (2006) The first structure of tyrosinase: All questions answered? *Angew. Chem., Int. Ed. 45*, 4546–4550.

BI8002764